J. Korean Math. Soc. **57** (2020), No. 5, pp. 1239–1266
https://doi.org/10.4134/JKMS.j190628
pISSN: 0304-9914 / eISSN: 2234-3008

MINIMAL LOCALLY STABILIZED *Q1-Q0* SCHEMES FOR THE GENERALIZED STOKES PROBLEM

Alima Chibani and Nasserdine Kechkar

Abstract. In this paper, some novel discrete formulations for stabilizing the mixed finite element method *Q1-Q0* (bilinear velocity and constant pressure approximations) are introduced and discussed for the generalized Stokes problem. These are based on stabilizing discontinuous pressure approximations via local jump operators. The developing idea consists in a reduction of terms in the local jump formulation, introduced earlier, in such a way that stability and convergence properties are preserved. The computer implementation aspects and numerical evaluation of these stabilized discrete formulations are also considered. For illustrating the numerical performance of the proposed approaches and comparing the three versions of the local jump methods alongside with the global jump setting, some obtained results for two test generalized Stokes problems are presented. Numerical tests confirm the stability and accuracy characteristics of the resulting approximations.

1. Introduction

The mixed finite element methods are widely used for the numerical solution of incompressible flow problems. Many of them involve the use of approximations for the unknown primitive variables (velocity and pressure) in the Galerkin methodology. However, it is widely known that the discrete velocity and pressure spaces cannot be chosen independently of each other. There is a compatibility condition, commonly called the Babuška-Brezzi stability condition, that needs to be satisfied if the resulting mixed approximation is to be effective.

For simplicity, low-order mixed approximation methods are preferred. Nevertheless, many of them are unstable in the standard Babuška-Brezzi sense. Among these, the mixed methods referred to as *Q1-Q0, P1-P0, P1-P1* and *Q1-Q1* are notorious. Hence, Boland and Nicolaides [2] have shown that the mixed finite element *Q1-Q0* does not satisfy the stability condition. In addition, Sani et al. [18,19] have demonstrated that for certain boundary conditions

Received September 12, 2019; Revised May 30, 2020; Accepted June 10, 2020.
2010 *Mathematics Subject Classification.* Primary 65N30, 65N12, 65N15, 76D07.
Key words and phrases. Finite elements, mixed methods, generalized Stokes problem, stabilization.

the method generates spurious pressure modes (called checkerboard modes) resulting in numerical instabilities in the approximate pressure.

As a result of that, several researchers have been interested in overcoming the need of satisfying the Babuška-Brezzi stability condition. The idea of such called stabilization was initially proposed in the pioneering work of Brezzi and Pitkaranta [4]. Later, Hughes and Franca [14] constructed a Stokes discrete formulation which ensures convergence of discrete solutions for any mixed approximation. For a discontinuous pressure approximation, the called universal stability can be achieved by the introduction of pressure jump terms into the standard Galerkin discrete formulation. However, for achieving the universal stability, these jump terms must control pressure jumps across all internal inter-element edges. In the early 1990s, Silvester and Kechkar suggested in [21] that a more robust way of stabilizing a mixed method based on discontinuous pressure consists in restricting the global jump operator of Hughes and Franca locally to a macro-element partitioning of the solution domain. Furthermore, Kechkar and Silvester in [15] showed that the local jump stabilization can restore optimal interpolation rates of convergence for the *Q1-Q0* and *P1-P0* methods. A key feature of the local jump stabilization is that a conventional macro-element implementation is possible, so that the new stabilized discrete formulation can be implemented into element-by-element iterative solution techniques. The stabilized mixed *Q1-Q0* and *P1-P0* methods introduced by Silvester and Kechkar [21] and then analyzed in [15] have been applied to Stokes equations in many applications (*see* [5, 12, 13, 16]) while stability with respect to aspect ratio has been restored in [1] using minimal constraints on the pressure space.

In this paper, some modifications of the local jump stabilization technique, discussed in [15] and [21], are proposed for the *Q1-Q0* mixed element when used for the discretization of the generalized Stokes problem. The latter is obtained through the introduction of an additional term to the classical Stokes problem. It occurs in the refined numerical modeling of most industrial incompressible fluid flows (*see* [6, 10, 20]). The added term can be taken as a Darcy term or may represent the time discretization of the evolution term in the unsteady-state Stokes problem. The present techniques consist in reducing the number of local jump terms in the discrete formulation to two jumps, and even to one jump in each 2×2 macro-element. Furthermore, the local jump framework can be, more easily, implemented into existing software codes. The well-posedness and convergence of the two new stabilized discrete formulations are theoretically established, whereas the robustness properties are exhibited through some computational test problems.

The rest of the paper is organized as follows. In the next section, the generalized Stokes problem is briefly presented along with its weak formulation. Then, the standard Galerkin formulation is derived and discussed. In the following section, the local jump stabilized formulation by means of the *Q1-Q0* mixed method is reviewed and the new formulations (local two-jump and one-jump) are introduced. Stability and convergence analysis is addressed to in the

fourth section. Then, numerical performance of the new techniques is assessed on some test problems and compared to those of the earlier (local and global) jump stabilization techniques in the last section. Finally, some concluding remarks are given.

2. The generalized Stokes problem and its discrete formulations

Let Ω be a bounded two-dimensional domain with a polygonal boundary $\partial\Omega$. Consider the incompressible generalized Stokes problem (GSP), also called the Brinkman model: Given a body force $\mathbf{f}$, find functions $\mathbf{u} = (u_1, u_2)$ and p defined in Ω such that

$$\begin{aligned} \alpha\,\mathbf{u} - \mu\,\Delta\mathbf{u} + \nabla p &= \mathbf{f} \ \text{ in } \ \Omega, \\ \operatorname{div}\mathbf{u} &= 0 \ \text{ in } \ \Omega, \\ \mathbf{u} &= \mathbf{g} \ \text{ on } \ \Gamma, \end{aligned}$$

where $\mathbf{u}$ is the fluid velocity, p the pressure, $\mu > 0$ the kinematic viscosity coefficient, $\mathbf{g}$ a prescribed velocity on the boundary $\Gamma = \partial\Omega$, and α a positive real number that may come from the time discretization of the evolution term $\frac{\partial \mathbf{u}}{\partial t}$ in the unsteady-state Stokes equations (*cf.* [6]). Typically, we have $\alpha >> 1$.

Following the well-known monograph [11], there exists $\mathbf{u}_0 \in H^1(\Omega)$ such that $\mathbf{u}_0 = \mathbf{g}$ on Γ and $div\,\mathbf{u}_0 = 0$ in Ω. Therefore, setting $\mathbf{U} = \mathbf{u} - \mathbf{u}_0$ gives the problem:

Find $\mathbf{U}$ and p defined in Ω such that

$$\begin{aligned} \alpha\,\mathbf{U} - \mu\,\Delta\,\mathbf{U} + \nabla p &= \mathbf{f} - \alpha\,\mathbf{u}_0 + \mu\,\Delta\mathbf{u}_0 \quad \text{in } \Omega, \\ \operatorname{div}\mathbf{U} &= 0 \quad \text{in } \Omega, \\ \mathbf{U} &= \mathbf{0} \quad \text{on } \Gamma. \end{aligned}$$

The problem can then be stated as follows:

Find $\mathbf{u} = (u_1, u_2)$ and p defined in Ω such that

$$\begin{aligned} \alpha\mathbf{u} - \mu\Delta\mathbf{u} + \nabla p &= \mathbf{f} \quad \text{in } \Omega, \\ \operatorname{div}\mathbf{u} &= 0 \quad \text{in } \Omega, \\ \mathbf{u} &= 0 \quad \text{on } \Gamma, \end{aligned} \tag{2.1}$$

where $\mathbf{u}$ is used instead of $\mathbf{U}$. Throughout the paper, the homogeneous Dirichlet condition in (2.1), called no-slip boundary condition, is considered here only for simplicity of presentation. Other boundary conditions can also be taken as it will be the case below in the numerical experiments.

First, let us introduce the function spaces:

$$\mathbf{V} = \left[H_0^1(\Omega)\right]^2 \qquad \text{and} \qquad P = L_0^2(\Omega) = \left\{ q \in L^2(\Omega);\ \int_\Omega q\,\mathrm{d}x = 0 \right\} \tag{2.2}$$

with $L^2(\Omega)$, $H^1(\Omega)$ and $H_0^1(\Omega) = \{v \in H^1(\Omega);\ v = 0 \ \text{ on } \Gamma\}$ being the usual Lebesgue and Sobolev spaces. Furthermore, we will denote by $\|\cdot\|_0$ and $\|\cdot\|_1$

the norms in $L^2(\Omega)$ and $H^1(\Omega)$ respectively whereas the usual semi-norms in $H^1(\Omega)$ and $H^2(\Omega)$ are given respectively by

$$|v|_1 = \|\nabla v\|_0 = \left(\left\| \frac{\partial v}{\partial x_1} \right\|_0^2 + \left\| \frac{\partial v}{\partial x_2} \right\|_0^2 \right)^{\frac{1}{2}} \text{ and } |v|_2 = \left(\sum_{i_1+i_2=2} \left\| \frac{\partial^2 v}{\partial x_1^{i_1}\, \partial x_2^{i_2}} \right\|_0^2 \right)^{\frac{1}{2}}.$$

The choice of the pressure function space in (2.2) is needed to ensure the uniqueness since it is clear from (2.1) that the pressure can be determined only up to an additive constant.

Then, a weak formulation of the generalized Stokes problem (2.1) is given as follows:

Find $(\mathbf{u}, p) \in \mathbf{V} \times P$ such that

$$\begin{aligned} &\alpha \int_\Omega \mathbf{u} \cdot \mathbf{v}\, \mathrm{d}x + \mu \int_\Omega \nabla \mathbf{u} \cdot \nabla \mathbf{v}\, \mathrm{d}x \\ &\qquad - \int_\Omega p \operatorname{div} \mathbf{v}\ \mathrm{d}x = \int_\Omega \mathbf{f} \cdot \mathbf{v}\, \mathrm{d}x \qquad \forall \mathbf{v} \in \mathbf{V}, \\ &\qquad - \int_\Omega q \operatorname{div} \mathbf{u}\ \mathrm{d}x = 0 \qquad \forall q \in P. \end{aligned} \tag{2.3}$$

Note that we have multiplied the second equation in (2.3) by minus one. The purpose of this is to get a symmetric formulation which will greatly simplify the discussion. Further, we can take the right-hand side $\mathbf{f}$ in $[L^2(\Omega)]^2$, although this space is not the largest function space for the data $\mathbf{f}$ such that (2.3) makes sense.

Following standard arguments from the classical theory of Babuška-Brezzi (*cf.* [11]), it can be shown that there is a unique solution $(\mathbf{u}, p)$ to the weak formulation (2.3).

Now, let h (> 0) be a mesh parameter. Adopting a conform mixed finite element method by using finite-dimensional subspaces $\mathbf{V}_h \subset \mathbf{V}$ and $P_h \subset P$, the standard Galerkin methodology yields the following approximate problem:

Find $(\mathbf{u}_h, p_h) \in \mathbf{V}_h \times P_h$ such that

$$\begin{aligned} &\alpha \int_\Omega \mathbf{u}_h \cdot \mathbf{v}\, \mathrm{d}x + \mu \int_\Omega \nabla \mathbf{u}_h \cdot \nabla \mathbf{v}\, \mathrm{d}x \\ &\qquad - \int_\Omega p_h \operatorname{div} \mathbf{v}\ \mathrm{d}x = \int_\Omega \mathbf{f} \cdot \mathbf{v}\, \mathrm{d}x \qquad \forall \mathbf{v} \in \mathbf{V}_h, \end{aligned} \tag{2.4}$$

$$- \int_\Omega q \operatorname{div} \mathbf{u}_h\ \mathrm{d}x = 0 \qquad \forall q \in P_h. \tag{2.5}$$

The domain Ω is subdivided into convex quadrilaterals such that the resulting partitioning τ_h is regular in the usual sense, i.e., for some positive constants $\sigma > 1$ and $0 < \varepsilon < 1$ we have

$$h_K \le \sigma \rho_K \quad \text{and} \quad |\cos \theta_{i,K}| \le \varepsilon \quad \forall K \in \tau_h, \tag{2.6}$$

where h_K is the diameter of the element K, ρ_K the diameter of the inscribed circle of K and $\theta_{i,K}$ $(i = 1, 2, 3, 4)$ are the angles of K. The mesh parameter h is explicitly given by

$$h = \max_{K \in \tau_h} h_K.$$

Furthermore, the *Q1-Q0* mixed method is the lowest order conforming quadrilateral approximation method and is characterized by the pair of finite-dimensional spaces $\{\mathbf{V}_h, P_h\}$ defined by

$$\mathbf{V}_h = \left\{ \mathbf{v} \in \mathbf{V} \cap \mathbf{C}^0(\Omega);\ \mathbf{v}|_K \in [Q_1(K)]^2 \quad \forall K \in \tau_h \right\} \tag{2.7}$$

and

$$P_h = \{ q \in P;\ q|_K \in Q_0(K) \quad \forall K \in \tau_h \}, \tag{2.8}$$

where $Q_1(K)$ is the space of iso-parametrically transformed bilinear functions in each K and $Q_0(K)$ is the space of constant functions in each K.

As it was pointed out above, it has been shown in [2] that the finite element space pair given by (2.7) and (2.8) does not satisfy the key discrete Babuška-Brezzi stability condition:

$$\exists\, \omega > 0 \qquad \forall q \in P_h \qquad \sup_{0 \neq \mathbf{v} \in \mathbf{V}_h} \frac{(q, \mathrm{div}\mathbf{v})}{|\mathbf{v}|_1} \geq \omega \, \|q\|_0. \tag{2.9}$$

In this respect, in [18] and [19] it has also been demonstrated that the method develops spurious pressure modes resulting in numerical instabilities in the approximate pressure for certain boundary conditions. This suggests that for one or a few, but not all, $q \in P_h$ we have:

$$\int_\Omega q \, \mathrm{div}\, \mathbf{v} \, \mathrm{d}x = 0 \qquad \forall \mathbf{v} \in \mathbf{V}_h. \tag{2.10}$$

On the other hand, Boland and Nicolaides have also shown in [3] that, in this case, there is a more important failure of (2.9). In particular, they established the existence of some $q \in P_h$ such that

$$C_1 \, h \|q\|_0 \leq \sup_{0 \neq \mathbf{v} \in \mathbf{V}_h} \frac{(q, \mathrm{div}\, \mathbf{v})}{|\mathbf{v}|_1} \leq C_2 \, h \|q\|_0 \tag{2.11}$$

which implies that $\omega = 0$ in (2.9).

However, it should also be worth noting that *Q1-Q0* mixed approximation is stable if some non-rectangular meshes are used (*cf.* [9]). Because of the complexity of the latter and despite (2.10) and (2.11), the use of *Q1-Q0* approximation on rectangular meshes is motivated by its computational convenience. For simplicity of presentation, only rectangular axis-parallel meshes of the domain Ω will be considered in the remainder of the paper. The results can be easily extended to more general quadrilateral meshes using standard isoparametric transformations.

3. Local stabilizations of the *Q1-Q0* mixed finite element

In order to overcome the major difficulty mentioned above, the discrete problem (2.4), (2.5) can be stabilized by introducing into the equation (2.5) a bounded symmetric bilinear form $C_h(\cdot,\cdot)$ which is positive semi-definite over $P_h \times P_h$. In so doing, this induces the modified discrete incompressibility constraint:

$$-\int_\Omega q \operatorname{div} \mathbf{u}_h \, \mathrm{d}x - C_h(p_h, q) = 0 \qquad \forall q \in P_h. \tag{3.1}$$

The motivation behind introducing the form $C_h(\cdot,\cdot)$ is the following result which provides a sufficient condition for the well-posedness of the new discrete problem (2.4), (3.1).

Theorem 3.1 (*cf.* [21])**.** *Assume that the form $C_h(\cdot,\cdot)$ satisfies the condition*:

$$\begin{cases} \text{For any } p_m \in P_h \text{ such that } \int_\Omega q\, div\mathbf{v} dx = 0 \ \forall \mathbf{v} \in \mathbf{V}_h, \text{we have} \\ C_h(p_m, p_m) = 0 \qquad \Longrightarrow \quad p_m = 0. \end{cases} \tag{3.2}$$

Then, the solution $(\mathbf{u}_h, p_h)$ of (2.4), (3.1) *is uniquely determined in $\mathbf{V}_h \times P_h$.*

One such way of stabilizing the *Q1-Q0* mixed method was introduced in [14] through the so-called global jump stabilization. It consists in introducing the following bilinear form $C_h(\cdot,\cdot)$ into the discrete formulation (3.1):

$$C_h(p_h, q) = \beta \sum_{e=1}^{N_e} h_e \int_{\Gamma^{(e)}} [|p_h|]_{\Gamma^{(e)}} \, [|q|]_{\Gamma^{(e)}} \, \mathrm{d}s. \tag{3.3}$$

Here, $[|\cdot|]_{\Gamma^{(e)}}$ is the jump operator across $\Gamma^{(e)}$ and $\beta(>0)$ is a stabilizing parameter. The summation runs over all interior inter-element edges $\{\Gamma^{(e)};\ e = 1, 2, \ldots, N_e\}$ with lengths h_e. The modified discrete incompressibility constraint is then:

$$-\textstyle\int_\Omega q \operatorname{div} \mathbf{u}_h \, \mathrm{d}x - \beta \displaystyle\sum_{e=1}^{N_e} h_e \int_{\Gamma^{(e)}} [|p_h|]_{\Gamma^{(e)}} \, [|q|]_{\Gamma^{(e)}} \, \mathrm{d}s = 0 \qquad \forall q \in P_h. \tag{3.4}$$

A general theoretical analysis is given in [14]. Later, it was demonstrated in [21] that the global jump stabilization can be effective in practice. However, a careful choice of the parameter β is required to keep the accuracy in the solution.

As it was discussed in [21], the global jump method could be simplified by modifying the discrete bilinear form (3.3) using macro-elements. For this end, assume that the elements in τ_h can be assembled into disjoint element paths (macro-elements) so that a macro-element partitioning $\mathcal{M}_h$ is constructed. Moreover, the notion of the equivalence macro-element classes which are topologically equivalent to a reference macro-element $\widehat{M}$ (*cf.* [21]) leads to the following macro-element internal regularity condition: there exists a constant

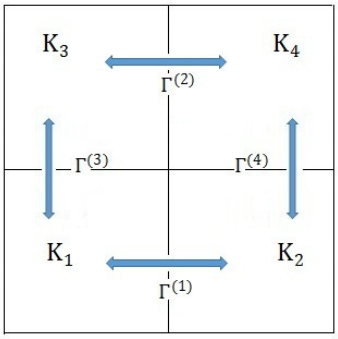

FIGURE 1. A 2×2 rectangular macro-element with four pressure jumps.

$\omega_{\widehat{M}} = \omega(\widehat{M}) > 0$ such that

$$K_M \geq \omega_{\widehat{M}}\, G_M, \tag{3.5}$$

where

$$G_M = \max_{K \subset M} |K|, \qquad K_M = \min_{K \subset M} |K|$$

and $|K|$ represents the area of K. In addition, suppose that the common boundary of any two neighboring macro-elements M_1, M_2 in $\mathcal{M}_h$ contains a node strictly in the interior of this boundary (connectivity macro-element condition). Then, the bilinear form C_h can be given, instead of (3.3), by

$$C_h(p_h, q) = \beta \sum_{M=1}^{N_M} \sum_{i=1}^{e_M} h_M^{(i)} \int_{\Gamma_M^{(i)}} [|p_h|]_{\Gamma_M^{(i)}}\, [|q|]_{\Gamma_M^{(i)}}\, \mathrm{d}s, \tag{3.6}$$

where the first summation is over all macro-elements, whereas the second summation runs over all inter-element edges strictly within each macro-element (see Figure 1 for a 2×2 rectangular macro-element). This stabilization technique will be referred to as the local jump stabilization.

Provided some usual smoothness and regularity assumptions on the solution $(\mathbf{u}, p)$ of (2.3), the following optimal error estimates for the Stokes problem ($\alpha = 0$) are theoretically established for the local jump stabilization in [15]:

$$\|\mathbf{u} - \mathbf{u}_h\|_1 + \|p - p_h\|_0 \leq C h\, (|\mathbf{u}|_2 + |p|_1), \tag{3.7}$$

$$\|\mathbf{u} - \mathbf{u}_h\|_0 \leq C\, h^2\, (|\mathbf{u}|_2 + |p|_1). \tag{3.8}$$

The arguments developed in [21] suggest that the local jump stabilization can be preferred to the global jump one because of its special features: (i) the

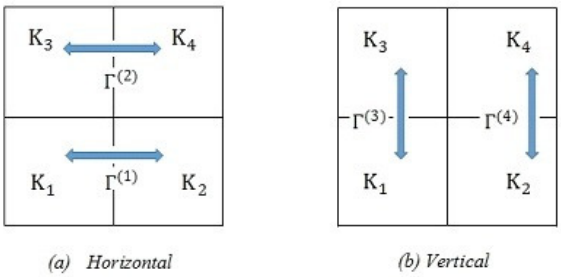

FIGURE 2. Two 2×2 rectangular macro-elements with two pressure jumps.

implementation is more straightforward since the local stabilization matrix obtained from (3.6) is block diagonal, (ii) the local mass conservation is preserved, (iii) the discrete velocity solution is less sensitive to the size of the stabilization parameter β.

Clearly, the two pressure jump stabilization techniques can be extended to the generalized Stokes problem (2.1) to get the error estimates (3.7) and (3.8) with the constant C depending on the parameter α as well.

In the remainder, for ensuring the connectivity macro-element condition mentioned above we assume that a coarser mesh $\mathcal{M}_h$ is given and that the latter is refined by joining the opposed element mid-edge points to get the grid τ_h. Next, two approaches for reduced local jump formulations will be presented. The well-posedness of the so-obtained discrete problem will be established in the next section.

3.1. Reduced local two-jump stabilizations

With preserved consistency and without apparently losing stability and convergence properties, the choice of (3.6) can be changed into a first reduced version by considering the pressure jumps only on one direction (horizontal or vertical) over inter-element edges strictly within each macro-element (*see* Figure 2).

The two new stabilized methods, which will be referred to as the reduced local two-jump stabilizations, are given by the bilinear form:

$$C_h^{(2)}(p_h, q) = \begin{cases} \beta \displaystyle\sum_{M=1}^{N_M} \sum_{i=1}^{2} h_M^{(i)} \int_{\Gamma_M^{(i)}} [|p_h|]_{\Gamma_M^{(i)}} \, [|q|]_{\Gamma_M^{(i)}} \, \mathrm{d}s \\ \text{or} \\ \beta \displaystyle\sum_{M=1}^{N_M} \sum_{i=3}^{4} h_M^{(i)} \int_{\Gamma_M^{(i)}} [|p_h|]_{\Gamma_M^{(i)}} \, [|q|]_{\Gamma_M^{(i)}} \, \mathrm{d}s. \end{cases} \tag{3.9}$$

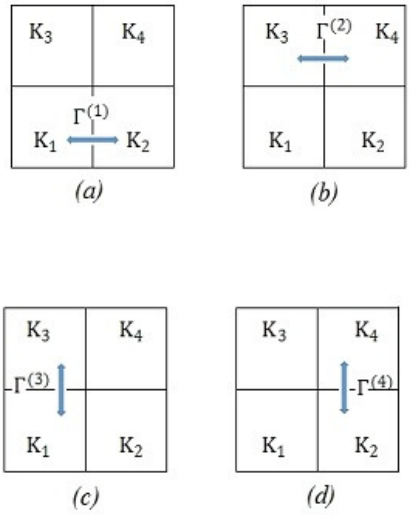

FIGURE 3. Four 2×2 rectangular macro-elements with one pressure jump.

This leads to the following perturbed discrete incompressibility constraint:

$$-\int_{\Omega} q \operatorname{div} \mathbf{u}_h \, \mathrm{d}x - C_h^{(2)}(p_h, q) = 0 \qquad \forall q \in P_h. \tag{3.10}$$

3.2. Reduced local one-jump stabilizations

Using 2×2 macro-elements, the reduced local two-jump formulations can themselves be simplified to the so-called reduced local one-jump formulations given by the stabilization bilinear forms:

$$C_h^{(1)}(p_h, q) = \beta \sum_{M=1}^{N_M} h_M \int_{\Gamma_M} [|p_h|]_{\Gamma_M} \, [|q|]_{\Gamma_M} \, \mathrm{d}s, \tag{3.11}$$

where Γ_M can be one of the four inter-element boundaries interior to the M-th macro-element. That is, the number of jumps within each macro-element is only one. Likewise, there is no jump over the macro-element boundaries (*see* Figure 3). This leads to the following perturbed discrete incompressibility constraint:

$$-\int_{\Omega} q \operatorname{div} \mathbf{u}_h \, \mathrm{d}x - C_h^{(1)}(p_h, q) = 0 \qquad \forall q \in P_h. \tag{3.12}$$

Remark 3.1. It should be mentioned that the idea of reducing the number of interior jumps in macro-elements can be naturally extended to three-dimensional *Q1-Q0* brick elements.

4. Stability and convergence analysis

First, let $B(\cdot,\cdot)$ be the generalized bilinear form

$$B\left((\mathbf{u},p);(\mathbf{v},q)\right)=\alpha\left(\mathbf{u},\mathbf{v}\right)+\mu\left(\nabla\mathbf{u},\nabla\mathbf{v}\right)-\left(p,\operatorname{div}\mathbf{v}\right)-\left(q,\operatorname{div}\mathbf{u}\right) \tag{4.1}$$

and $L(\cdot,\cdot)$ be the linear functional

$$L\left(\mathbf{v},q\right)=\left(\mathbf{f},\mathbf{v}\right), \tag{4.2}$$

where $(\cdot,\cdot)$ denotes the usual L^2-inner product. Thus, the problem (2.3) can be restated as:

$$\text{Find } (\mathbf{u},p)\in\mathbf{V}\times P \text{ such that}$$

$$B\left((\mathbf{u},p);(\mathbf{v},q)\right)=L\left(\mathbf{v},q\right)\qquad\forall\left(\mathbf{v},q\right)\in\mathbf{V}\times P. \tag{4.3}$$

Next, for all $(\mathbf{v},q)\in\mathbf{V}_h\times P_h$ by setting

$$\begin{cases} B_h\left((\mathbf{u}_h,p_h);(\mathbf{v},q)\right)=\alpha\left(\mathbf{u}_h,\mathbf{v}\right)+\mu\left(\nabla\mathbf{u}_h,\nabla\mathbf{v}\right)-\left(p_h,\operatorname{div}\mathbf{v}\right) \\ \qquad\qquad\qquad\qquad -\left(q,\operatorname{div}\mathbf{u}_h\right), \\ L_h\left(\mathbf{v},q\right)=\left(\mathbf{f},\mathbf{v}\right) \end{cases} \tag{4.4}$$

and by introducing the bilinear form

$$C_h^{(t)}\left(r,q\right)=\begin{cases} C_h^{(2)}\left(r,q\right) & \text{for the reduced local two-jump formulations,} \\ C_h^{(1)}\left(r,q\right) & \text{for the reduced local one-jump formulations,} \end{cases} \tag{4.5}$$

for all $r,q\in P_h$, where $C_h^{(2)}(\cdot,\cdot)$ and $C_h^{(1)}(\cdot,\cdot)$ are defined in (3.9) and (3.11) respectively, the reduced locally stabilized formulations (2.4), (3.10) and (2.4), (3.12) become:

$$\text{Find } (\mathbf{u},p)\in\mathbf{V}\times P \text{ such that}$$

$$B_h^{(t)}\left((\mathbf{u}_h,p_h);(\mathbf{v},q)\right)=L_h\left(\mathbf{v},q\right)\qquad\forall\left(\mathbf{v},q\right)\in\mathbf{V}_h\times P_h, \tag{4.6}$$

where

$$B_h^{(t)}\left((\mathbf{u}_h,p_h);(\mathbf{v},q)\right)=B_h\left((\mathbf{u}_h,p_h);(\mathbf{v},q)\right)-\beta C_h^{(t)}\left(p_h,q\right) \tag{4.7}$$

for $t=1,2$.

We also need to define some subspaces of the discrete pressure space P_h. Set

$$R_h=\begin{cases} \{q\in P_h;\ [|q|]_{\Gamma_M^{(1)}}=[|q|]_{\Gamma_M^{(2)}}=0\quad\forall M\in\mathcal{M}_h\} & \text{for 2-jump H,} \\ \{q\in P_h;\ [|q|]_{\Gamma_M^{(3)}}=[|q|]_{\Gamma_M^{(4)}}=0\quad\forall M\in\mathcal{M}_h\} & \text{for 2-jump V,} \\ \{q\in P_h;\ [|q|]_{\Gamma_M^{(1)}}=0\quad\forall M\in\mathcal{M}_h\} & \text{for 1-jump H1,} \\ \{q\in P_h;\ [|q|]_{\Gamma_M^{(2)}}=0\quad\forall M\in\mathcal{M}_h\} & \text{for 1-jump H2,} \\ \{q\in P_h;\ [|q|]_{\Gamma_M^{(3)}}=0\quad\forall M\in\mathcal{M}_h\} & \text{for 1-jump V1,} \\ \{q\in P_h;\ [|q|]_{\Gamma_M^{(4)}}=0\quad\forall M\in\mathcal{M}_h\} & \text{for 1-jump V2.} \end{cases} \tag{4.8}$$

Now, let $C_M^{(t)}(\cdot,\cdot)$ be the restriction of $C_h^{(t)}(\cdot,\cdot)$ to a macro-element M. Hence, $C_M^{(2)}(\cdot,\cdot)$ and $C_M^{(1)}(\cdot,\cdot)$ are the restrictions to a macro-element M of $C_h^{(2)}(\cdot,\cdot)$ and $C_h^{(1)}(\cdot,\cdot)$ respectively, i.e.,

$$C_M^{(2)}(r,q) = \begin{cases} \beta \sum_{i=1}^{2} h_M^{(i)} \int_{\Gamma_M^{(i)}} [|p_h|]_{\Gamma_M^{(i)}} \, [|q|]_{\Gamma_M^{(i)}} \, \mathrm{d}s \\ \text{or} \\ \beta \sum_{i=3}^{4} h_M^{(i)} \int_{\Gamma_M^{(i)}} [|p_h|]_{\Gamma_M^{(i)}} \, [|q|]_{\Gamma_M^{(i)}} \, \mathrm{d}s \end{cases} \tag{4.9}$$

and

$$C_M^{(1)}(r,q) = \beta \, h_M \int_{\Gamma_M} [|r|]_{\Gamma_M} \, [|q|]_{\Gamma_M} \mathrm{d}s \tag{4.10}$$

for all $r, q \in P_h$.

For $t = 1, 2$ we obviously have

$$C_h^{(t)}(r,q) = \sum_{M=1}^{N_M} C_M^{(t)}(r,q) \qquad \forall r, q \in P_h. \tag{4.11}$$

Moreover, the restricted pressure spaces for a macro-element M are given by

$$P_{0,M} = \left\{ q \in L_0^2(M) \,;\, q_{|_K} \text{ is constant } \forall K \subset M \right\}, \quad R_M = L_0^2(M) \cap R_h, \tag{4.12}$$

accordingly to (4.8).

For analyzing the stability of the proposed local (two-jump or one-jump) stabilized formulations, we first establish two interesting lemmas. The first one gives a macro-element positivity of the stabilization bilinear form $C_h^{(t)}(\cdot,\cdot)$.

Lemma 4.1. *Let $\zeta_{\widehat{M}}$ be a class of equivalent macro-elements. Then, there exists $\gamma_{\widehat{M}} > 0$ such that*

$$C_M^{(t)}(q,q) \geq \gamma_{\widehat{M}} \|q\|_{0,M}^2 \qquad \forall q \in P_{0,M} \setminus R_M \tag{4.13}$$

for $t = 1, 2$.

Proof. Let $M \in \zeta_{\widehat{M}}$ and $q \in P_{0,M} \setminus R_M$. From the definition (4.9) or (4.10) of $C_M^{(t)}$, we first note that $C_M^{(t)}(q,q) = 0$ if and only if $q \in R_M$. Hence, the constant γ_M defined through

$$\gamma_M = \inf_{\substack{q \in P_{0,M} \setminus R_M \\ \|q\|_{0,M} = 1}} C_M^{(t)}(q,q) \tag{4.14}$$

is positive. By virtue of a scaling argument (*cf.* [22]), the regularity assumptions (2.6) guarantee the existence of a constant $\gamma_{\widehat{M}}$ such that

$$\gamma_M \geq \gamma_{\widehat{M}} > 0 \qquad \forall M \in \zeta_{\widehat{M}}$$

which implies (4.13). □

Next, let us assume that there is a fixed set of classes $\zeta_{\widehat{M}_i}$, $i = 1, 2, \ldots, n$ ($n \geq 1$) such that every macro-element $M \in \mathcal{M}_h$ belongs to one of the equivalence classes. Denote by $\Lambda_h : P_h \longrightarrow R_h$ an L^2-projection from P_h onto its subspace R_h. A direct consequence of the last lemma is the following global positivity of the form $C_h^{(t)}$:

$$C_h^{(t)}(q,q) \geq \alpha_1 \| (I - \Lambda_h) q \|_0^2 \qquad \forall q \in P_h \tag{4.15}$$

with

$$\alpha_1 = \min\{\gamma_{\widehat{M}_i} : i = 1, 2, \ldots, n\}$$

which is independent of h for $t = 1, 2$. The proof of this is based on (4.13) combined with the following obvious identity:

$$C_M^{(t)}(q,q) = C_M^{(t)}((I - \Lambda_h)q, (I - \Lambda_h)q) \qquad \forall q \in P_h, \tag{4.16}$$

since the jump $[|\Lambda_h q|]$ vanishes within M as $\Lambda_h q \in R_h$.

The second lemma is a global stability result for the discrete pressure space R_h.

Lemma 4.2. *There exists a positive constant α_2 independent of h such that for every $q \in P_h$ there is a $\mathbf{g}_h \in \mathbf{V}_h$ satisfying*

$$(\Lambda_h q, div\, \mathbf{g}_h) = \|\Lambda_h q\|_0^2 \qquad and \qquad \|\mathbf{g}_h\|_1 \leq \alpha_2 \|\Lambda_h q\|_0. \tag{4.17}$$

Proof. Let $q \in P_h$ be arbitrary. Since $\Lambda_h q \in R_h \subset L_0^2(\Omega)$ there exist $C_1 > 0$ and $\mathbf{g} \in \mathbf{V}$ such that (*cf.* [11])

$$\operatorname{div} \mathbf{g} = \Lambda_h q \qquad \text{and} \qquad \|\mathbf{g}\|_1 \leq C_1 \|\Lambda_h q\|_0. \tag{4.18}$$

We can combine some ideas from [7] and [8] with the macro-element methodology of [22] in order to construct an operator $I_h : \mathbf{V} \longrightarrow \mathbf{V}_h$ such that

$$(\operatorname{div} I_h \mathbf{g}, r) = (\operatorname{div} \mathbf{g}, r) \quad \forall r \in P_h \qquad \text{and} \qquad \|I_h \mathbf{g}\|_1 \leq C_2 \|\mathbf{g}\|_1.$$

It remains to take $\mathbf{g}_h = I_h \mathbf{g}$ and $\alpha_2 = C_1 C_2$. □

Now, we are in a position to state the following main inf-sup result which ensures the well-posedness of the discrete formulation (4.6).

Theorem 4.1. *There exists a constant $\gamma > 0$ independent of the mesh parameter h such that*

$$\sup_{(\mathbf{w},r) \in \mathbf{V}_h \times P_h} \frac{B_h^{(t)}((\mathbf{v},q);\,(\mathbf{w},r))}{\|\mathbf{w}\|_1 + \|r\|_0} \geq \gamma \left(\|\mathbf{v}\|_1 + \|q\|_0\right) \quad \forall (\mathbf{v},q) \in \mathbf{V}_h \times P_h. \tag{4.19}$$

Proof. Let $(\mathbf{v},q) \in \mathbf{V}_h \times P_h$ and $\alpha_1$be as in (4.15). Set $r = -q$, $\mathbf{w} = \mathbf{v} - \delta\, \mathbf{g}_h$, where δ is a positive constant to be determined below. From (4.15) and (4.17), it follows that

$$\begin{aligned} B_h^{(t)}((\mathbf{v},q);(\mathbf{w},r)) = {} & \alpha(\mathbf{v},\mathbf{v}) - \delta\alpha(\mathbf{v},\mathbf{g}_h) + \mu(\nabla\mathbf{v},\nabla\mathbf{v}) - \delta\mu(\nabla\mathbf{v},\nabla\mathbf{g}_h) \\ & + \delta(q, \operatorname{div}\mathbf{g}_h) + \beta C_h^{(t)}(q,q) \end{aligned}$$

$$
\begin{aligned}
&= \alpha\|\mathbf{v}\|_0^2 + \mu\|\nabla\mathbf{v}\|_0^2 - \delta\alpha(\mathbf{v},\mathbf{g}_h) - \delta\mu(\nabla\mathbf{v},\nabla\mathbf{g}_h)\\
&\quad + \delta(\Lambda_h q, \mathrm{div}\mathbf{g}_h) - \delta((\Lambda_h - I)q, \mathrm{div}\mathbf{g}_h) + \beta C_h^{(t)}\ (q,q)\\
&\geq \alpha\|\mathbf{v}\|_0^2 + \mu\|\nabla\mathbf{v}\|_0^2 - \delta\alpha\alpha_2\|\mathbf{v}\|_0\|\Lambda_h q\|_0\\
&\quad - \delta\mu\alpha_2\|\nabla\mathbf{v}\|_0\|\Lambda_h q\|_0 + \delta\|\Lambda_h q\|_0^2\\
&\quad - \delta\alpha_2\|(\Lambda_h - I)q\|_0\|\Lambda_h q\|_0 + \beta\alpha_1\|(I-\Lambda_h)q\|_0^2\\
&\geq \alpha\|\mathbf{v}\|_0^2 + \mu\|\nabla\mathbf{v}\|_0^2 - \frac{\alpha}{2}(\|\mathbf{v}\|_0^2 + \delta^2\alpha_2^2\|\Lambda_h q\|_0^2)\\
&\quad - \frac{\mu}{2}(\|\nabla\mathbf{v}\|_0^2 + \delta^2\alpha_2^2\|\Lambda_h q\|_0^2) + \delta\|\Lambda_h q\|_0^2\\
&\quad - \frac{\beta\alpha_1}{2}[\|(\Lambda_h - I)q\|_0^2 + (\frac{\delta\alpha_2}{\beta\alpha_1})^2\|\Lambda_h q\|_0^2]\\
&\quad + \beta\alpha_1\|(I-\Lambda_h)q\|_0^2.
\end{aligned}
$$

By choosing $\delta = \frac{1}{\alpha_2^2}\left(\frac{1}{\beta\alpha_1} + \alpha + \mu\right)^{-1}$, we get

$$
B_h^{(t)}((\mathbf{v},q);(\mathbf{w},r)) \geq \frac{\alpha}{2}\|\mathbf{v}\|_0^2 + \frac{\mu}{2}\|\nabla\mathbf{v}\|_0^2 + \frac{\beta\alpha_1}{2}\|(I-\Lambda_h)q\|_0^2 + \frac{\delta}{2}\|\Lambda_h q\|_0^2
$$

which implies that

$$
B_h^{(t)}((\mathbf{v},q);(\mathbf{w},r)) \geq \kappa_1(\|\mathbf{v}\|_1 + \|q\|_0)^2, \tag{4.20}
$$

where $\kappa_1 = \frac{1}{4}\min\{\alpha,\mu,\beta\alpha_1,\delta\}$.

On the other hand, we have

$$
\begin{aligned}
\|\mathbf{w}\|_1 + \|r\|_0 &= \|\mathbf{v} - \delta\,\mathbf{g}_h\|_1 + \|q\|_0\\
&\leq \|\mathbf{v}\|_1 + \delta\|\mathbf{g}_h\|_1 + \|q\|_0\\
&\leq \|\mathbf{v}\|_1 + \delta\alpha_2\|\Lambda_h q\|_0 + \|q\|_0\\
&\leq \kappa_2(\|\mathbf{v}\|_1 + \|q\|_0), \qquad (4.21)
\end{aligned}
$$

where $\kappa_2 = 1+\delta\alpha_2$. Finally, combining (4.19) and (4.20) establishes the desired inequality (4.18) with $\gamma = \frac{\kappa_1}{\kappa_2}$. □

Next, let us state two important interpolation results which are required below (*cf.* [11]).

Lemma 4.3. *If $\mathbf{v} \in [H^2(\Omega)\cap H_0^1(\Omega)]^2$, then there exists $\tilde{\mathbf{v}} \in \mathbf{V}_h$ such that*

$$
\|\mathbf{v} - \tilde{\mathbf{v}}\|_1 \leq C_1 h|\mathbf{v}|_2, \tag{4.22}
$$

where C_1 is a constant independent of h.

Lemma 4.4. *If $q \in H^1(\Omega)\cap L_0^2(\Omega)$, then there exists $\tilde{q} \in R_h$ such that*

$$
\|q - \tilde{q}\|_1 \leq C_2 h|q|_1, \tag{4.23}
$$

where C_2 is a constant independent of h.

The convergence of the proposed stabilization schemes is given by the optimal error estimate shown in the following theorem.

Theorem 4.2. *Suppose that the solution of* (4.3) *satisfies* $\mathbf{u} \in [H^2(\Omega)]^2$ *and* $p \in H^1(\Omega)$. *Then, there exists a constant* C *independent of* h *such that*

$$\|\mathbf{u} - \mathbf{u}_h\|_1 + \|p - p_h\|_0 \leq Ch(|\mathbf{u}|_2 + |p|_1), \tag{4.24}$$

where $(\mathbf{u}_h, p_h)$ *is the solution of* (4.6).

Proof. Applying (4.3) and (4.4) with $\mathbf{v} = \mathbf{u}$ and $q = p$ respectively, there exist $\tilde{\mathbf{u}} \in \mathbf{V}_h$ and $\tilde{p} \in R_h$ such that (4.22) and (4.23) hold. Then,

$$\begin{aligned} B_h^{(t)}\left((\mathbf{u}_h - \tilde{\mathbf{u}}, p_h - \tilde{p})\,;\,(\mathbf{v}, q)\right) &= B_h^{(t)}\left((\mathbf{u}_h, p_h)\,;(\mathbf{v}, q)\right) - B_h^{(t)}\left((\tilde{\mathbf{u}}, \tilde{p})\,;(\mathbf{v}, q)\right) \\ &= B_h^{(t)}\left((\mathbf{u}_h, p_h)\,;(\mathbf{v}, q)\right) - B\left((\tilde{\mathbf{u}}, \tilde{p})\,;(\mathbf{v}, q)\right), \end{aligned} \tag{4.25}$$

since $\tilde{p} \in R_h$ so that $C_h^{(t)}(\tilde{p}, q) = 0$. Moreover, we have

$$B_h^{(t)}\left((\mathbf{u}_h, p_h)\,;(\mathbf{v}, q)\right) = L_h(\mathbf{v}, q) = B\left((\mathbf{u}, p)\,;(\mathbf{v}, q)\right), \tag{4.26}$$

because $L_h(\mathbf{v}, q) = L(\mathbf{v}, q)$ for all $(\mathbf{v}, q) \in \mathbf{V}_h \times P_h$. Next, (4.25) yields

$$\begin{aligned} B_h^{(t)}\left((\mathbf{u}_h - \tilde{\mathbf{u}}, p_h - \tilde{p})\,;(\mathbf{v}, q)\right) &= B\left((\mathbf{u} - \tilde{\mathbf{u}}, p - \tilde{p})\,;(\mathbf{v}, q)\right) \\ &\leq \alpha\|\mathbf{u} - \tilde{\mathbf{u}}\|_1\|\mathbf{v}\|_1 + \mu\|\mathbf{u} - \tilde{\mathbf{u}}\|_1\|\mathbf{v}\|_1 \\ &\quad + \|\mathbf{u} - \tilde{\mathbf{u}}\|_1\|q\|_0 + \|p - \tilde{p}\|_0\|\mathbf{v}\|_1 \\ &\leq C_3\left(\|\mathbf{u} - \tilde{\mathbf{u}}\|_1 + \|p - \tilde{p}\|_0\right)\left(\|\mathbf{v}\|_1 + \|q\|_0\right) \end{aligned} \tag{4.27}$$

for all $(\mathbf{v}, q) \in \mathbf{V}_h \times P_h$, where $C_3 = \max\{\alpha, \mu, 1\}$. Thus,

$$\sup_{(\mathbf{v},q)\in\mathbf{V}_h\times P_h} \frac{B\left((\mathbf{u} - \tilde{\mathbf{u}}, p - \tilde{p})\,;(\mathbf{v}, q)\right)}{\|\mathbf{v}\|_1 + \|q\|_0} \leq C_3\left(\|\mathbf{u} - \tilde{\mathbf{u}}\|_1 + \|p - \tilde{p}\|_0\right) \tag{4.28}$$

so that (4.26) yields

$$\sup_{(\mathbf{v},q)\in\mathbf{V}_h\times P_h} \frac{B_h^{(t)}\left((\mathbf{u}_h - \tilde{\mathbf{u}}, p_h - \tilde{p})\,;(\mathbf{v}, q)\right)}{\|\mathbf{v}\|_1 + \|q\|_0} \leq C_3\left(\|\mathbf{u} - \tilde{\mathbf{u}}\|_1 + \|p - \tilde{p}\|_0\right).$$

From (4.19), it follows that

$$\|\mathbf{u}_h - \tilde{\mathbf{u}}\|_1 + \|p_h - \tilde{p}\|_0 \leq \frac{C_3}{\gamma}\left(\|\mathbf{u} - \tilde{\mathbf{u}}\|_1 + \|p - \tilde{p}\|_0\right).$$

Therefore,

$$\|\mathbf{u} - \mathbf{u}_h\|_1 + \|p - p_h\|_0 \leq \left(1 + \frac{C_3}{\gamma}\right)\left(\|\mathbf{u} - \tilde{\mathbf{u}}\|_1 + \|p - \tilde{p}\|_0\right).$$

Consequently, applying (4.22) and (4.23) gives the desired inequality (4.24) where the constant C is given by

$$C = \max\{C_1, C_2\}\left(1 + \frac{C_3}{\gamma}\right).$$

□

Remark 4.1. It is instructive to note that substituting for the value of γ given in the proof of 4.1, the constant C takes the form:

(4.29)
$$C = \max\{C_1, C_2\}\left(1 + 4\max\{\alpha,\mu,1\}\frac{1+\frac{1}{\alpha_2\left(\alpha+\mu+\frac{1}{\beta\alpha_1}\right)}}{\min\left\{\alpha,\mu,\beta\alpha_1,\frac{1}{\alpha_2^2\left(\alpha+\mu+\frac{1}{\beta\alpha_1}\right)}\right\}}\right).$$

This shows, to some extent, that the convergence can be influenced by the values of α and μ. If α is very large and/or μ is too small, then this can compromize the approximation accuracy especially for practical values of h.

Remark 4.2. According to the inequality (4.24), the convergence of the discrete solution $(\mathbf{u}_h, p_h)$ given by (4.6) to $(\mathbf{u}, p)$ is then guaranteed since

$$\lim_{h\to 0}(\|\mathbf{u}-\mathbf{u}_h\|_1 + \|p-p_h\|_0) = 0.$$

Remark 4.3. Assuming, for instance, that for any $\mathbf{f} \in [L^2(\Omega)]^2$ the corresponding solution $(\mathbf{u}, p)$ of (2.3) satisfies the inequality:

$$\|\mathbf{u}\|_2 + \|p\|_1 \leq \epsilon\|\mathbf{f}\|_0, \tag{4.30}$$

with $\epsilon > 0$, the use of a dual problem allows to prove the following optimal L_2-error estimate for the velocity:

$$\|\mathbf{u}-\mathbf{u}_h\|_0 \leq \theta\, h^2(|\mathbf{u}|_2 + |p|_1), \tag{4.31}$$

where θ is a certain constant independent of h.

5. Numerical experiments

In this section, the numerical performance of the two reduced local jump stabilization procedures is assessed and compared with that of the global and local jump methods. We consider two computational test problems specifically chosen to illustrate the different features of the new methods.

First, for problem discretization, the domain is uniformly subdivided ($h = h_x = h_y$) into square elements generating the sequence of grids GR0, GR1, GR8 with respective sizes $h = 2^{-i}$ $(i = 1, \ldots, 9)$.

Many fixed values of the stabilization parameter β were considered. However, we present only the representative cases β=1 and β=100. It is worth to mention that more investigation is still underway to determine any optimal value of β. In all present numerical tests, the kinematic viscosity coefficient μ was set to be 1, whereas the parameter α is considered to be 10^n, $n \in \{0, 1, 2, 3\}$.

In addition, if not properly specified, the reported results will concern mainly the global and local jump schemes together with the horizontal 2-jump (2-jp H) and the vertical 1-jump (1-jp V1) schemes in the first test problem, and

together with the vertical 2-jump (2-jp V) and the horizontal 1-jump (1-jp H2) schemes in the second test problem. In each case, some other results will also concern the remaining schemes and are used for comparison purposes.

All computations and figure generations were performed in Matlab on a Intel(R) Core(TM) i5 PC @ 2.53MHz.

5.1. Problem with an analytical solution

This first problem is used as a study of convergence rates and comparison of the different methods in terms of accuracy. The problem is that of an enclosed flow in the unit square $\Omega = [0,1] \times [0,1]$ with the velocity vector and pressure solution fields being given by:

$$\mathbf{u}(x,y) = \begin{bmatrix} x^2\left(\frac{x}{3} - \frac{1}{2}\right) \\ \\ xy(1-x) \end{bmatrix}, \qquad p(x,y) = x^2 - \frac{1}{3} \tag{5.1}$$

which clearly satisfies the constraint $\int_\Omega p(x,y)d\Omega = 0$. The body force $\mathbf{f}$ is then chosen to satisfy (2.1). The values of $\mathbf{u}$ on the boundary of Ω are constrained to those given above. Furthermore, in order to ensure the zero average condition ($P_h \subset L^2_0(\Omega)$), the pressure is fixed at a given point of the domain Ω, or more precisely, a pressure nodal value has been imposed (*cf.* [18]).

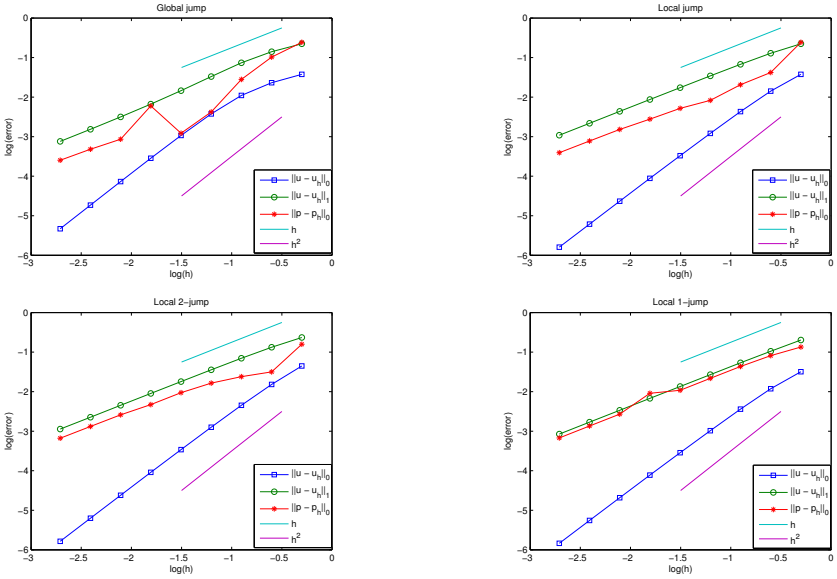

FIGURE 4. Convergence history for β=1 and α=1.

An analysis of the results, displayed in Figures 4-6, shows that for all considered values of α the rates of convergence behave as predicted by the theory,

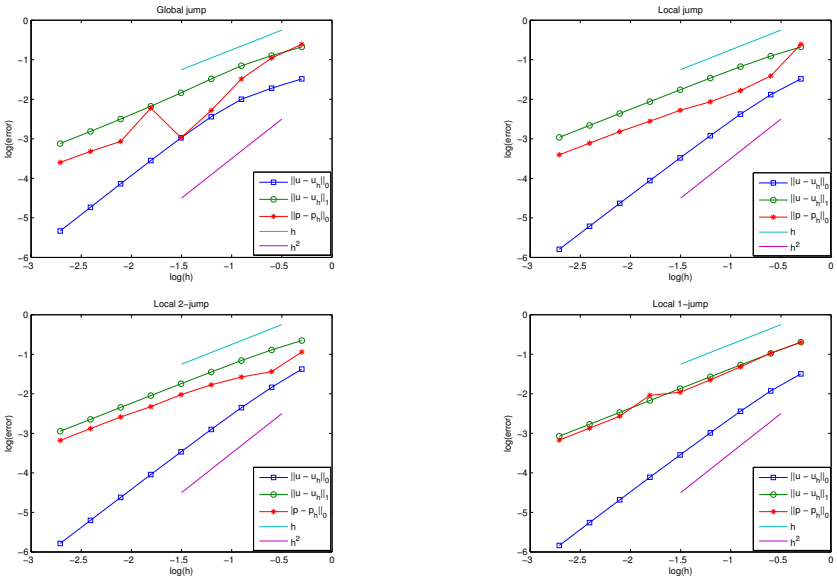

FIGURE 5. Convergence history for β=1 and α=10.

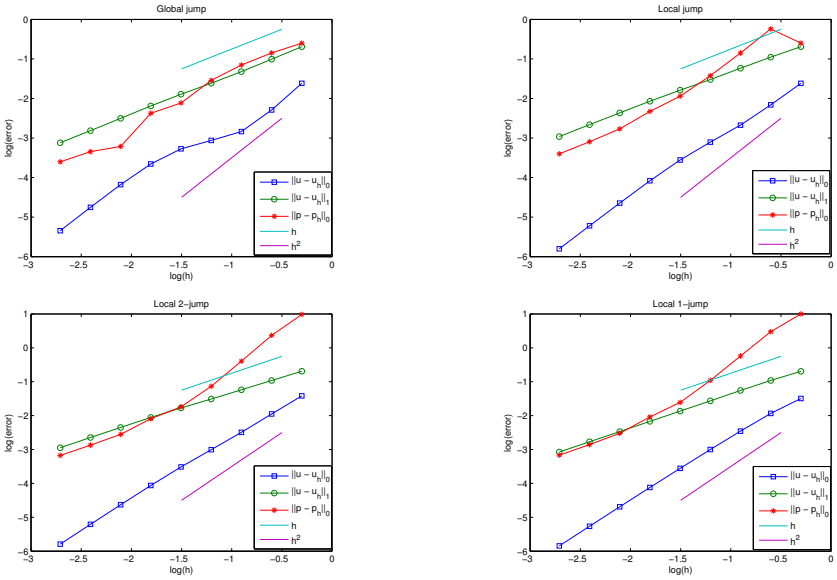

FIGURE 6. Convergence history for β=1 and α=1000.

i.e., $O(h)$ order of convergence for $\|\mathbf{u}-\mathbf{u}_h\|_1$ and $\|p-p_h\|_0$, and $O(h^2)$ order of convergence for $\|\mathbf{u}-\mathbf{u}_h\|_0$. This occurs for all stabilized schemes except the global jump one for which we notice no monotonic decrease for the pressure errors. On the other hand, due to the constant C in Theorem 4.2 given by (4.29), some of these rates begin to deteriorate as α takes values above 1000.

TABLE 1. Comparison of $\|\mathbf{u}-\mathbf{u}_h\|_0$ results for β=1 as α grows.

α	**Global jump**	**Local jump**	**Local 2-jump**	**Local 1-jump**
0	4.688920E − 6	1.603484E − 6	1.641443E − 6	1.459032E − 6
1	4.687322E − 6	1.603166E − 6	1.641484E − 6	1.458766E − 6
10	4.672607E − 6	1.603220E − 6	1.639725E − 6	1.457984E − 6
100	4.606065E − 6	1.594786E − 6	1.633302E − 6	1.450797E − 6
1000	4.512608E − 6	1.576241E − 6	1.615563E − 6	1.432673E − 6

TABLE 2. Comparison of $\|\mathbf{u}-\mathbf{u}_h\|_1$ results for β=1 as α grows.

α	**Global jump**	**Local jump**	**Local 2-jump**	**Local 1-jump**
0	7.574209E − 4	1.088619E − 3	1.128951E − 3	8.450228E − 4
1	7.574209E − 4	1.088624E − 3	1.128951E − 3	8.450183E − 4
10	7.574196E − 4	1.088699E − 3	1.128949E − 3	8.450195E − 4
100	7.574232E − 4	1.088581E − 3	1.128925E − 3	8.450167E − 4
1000	7.574430E − 4	1.088217E − 3	1.128567E − 3	8.450544E − 4

TABLE 3. Comparison of $\|p-p_h\|_0$ results for β=1 as α grows.

α	**Global jump**	**Local jump**	**Local 2-jump**	**Local 1-jump**
0	2.527735E − 4	3.932066E − 4	6.625991E − 4	6.762094E − 4
1	2.527683E − 4	3.932277E − 4	6.626018E − 4	6.762154E − 4
10	2.527273E − 4	3.936559E − 4	6.626364E − 4	6.762573E − 4
10^2	2.524362E − 4	3.936708E − 4	6.631283E − 4	6.768359E − 4
10^3	2.496844E − 4	3.974746E − 4	6.672416E − 4	6.824065E − 4

Furthermore, in order to show the sensitivity of L^2 and H^1 velocity errors, and L^2 pressure errors to the choice of the parameter α, the results are depicted in Tables 1-3 for the finest mesh GR8 with uniform size h=2^{-9} and the stabilization parameter β=1. As may be seen, the error magnitudes are not so affected by the increase of α. It is important to mention that the local 2-jump and 1-jump schemes perform remarkably well. The velocity results of the 1-jump scheme are even better than those of the local jump method. When

analyzing for other considered values of β, not reported here, we also noticed the sensitivity of the global jump scheme to the value of β, confirming what was claimed above. This fact will be more illustrated next.

5.2. Lid-driven cavity problem

The generalized Stokes problem (GSP) with $\mathbf{f} = \mathbf{0}$ is to be solved in the unit square $[0,1] \times [0,1]$ with the imposed non leaky boundary conditions:

$$\begin{aligned} \mathbf{u}(0,y) = \mathbf{u}(1,y) = \mathbf{u}(x,0) &= \mathbf{0} \qquad \text{if } 0 \le x, y \le 1, \\ \mathbf{u}(x,1) &= [1\ 0]^T \qquad \text{if } 0 < x < 1. \end{aligned} \tag{5.2}$$

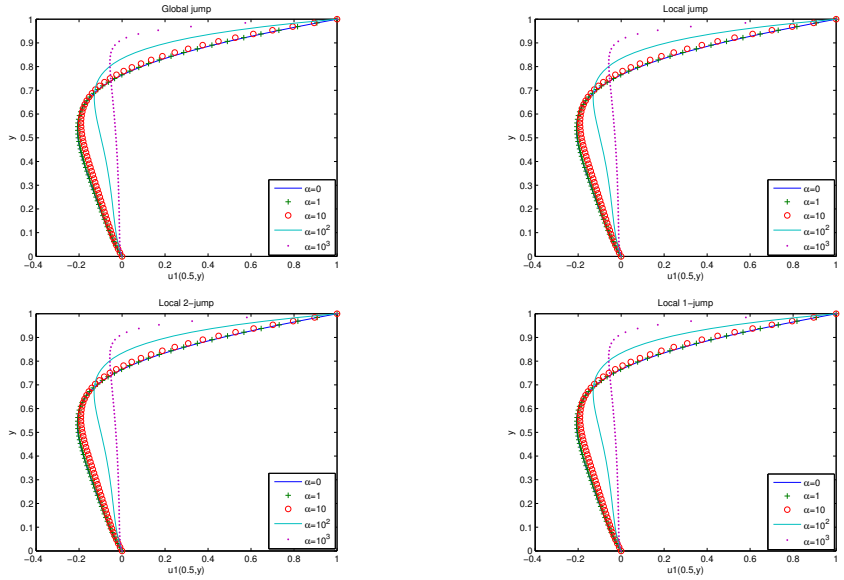

FIGURE 7. Horizontal velocity profiles for β=1 when α grows.

In order to assess the performance of the local jump stabilization techniques and compare them with the local jump and global jump methods, the mesh GR5 with uniform size h=2^{-6} is used. Owing to the fact that the lid-driven cavity problem does not possess an analytic solution, it is generally impossible to calculate the exact accuracy and hence the convergence rates for the discrete solutions. Fortunately, there are features that can be exhibited to give an idea of how the computed solutions behave.

First, the convergence of the velocity can be assessed by plotting the profiles of the horizontal velocity u_1 along the centerline ($x = 0.5$). The obtained profiles are depicted in Figures 7-8. As can be seen from these figures, the local 2-jump and 1-jump schemes perform well and reproduce profiles which are almost indistinguishable with those of the local jump. However, as can be seen

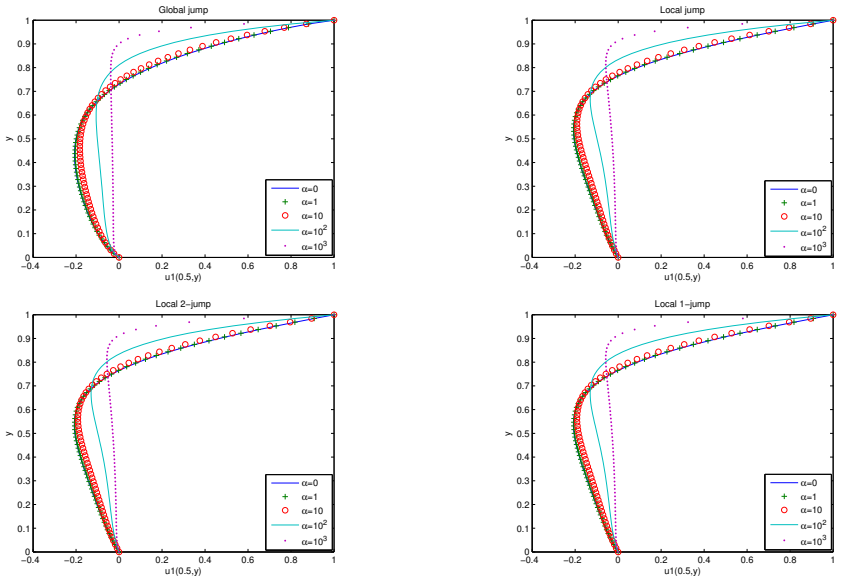

FIGURE 8. Horizontal velocity profiles for β=100 when α grows.

the global jump technique can yield very inaccurate velocity solutions when the stabilization parameter β is varied. This demonstrates once more that the jump locally stabilized schemes are far less sensitive to the choice of β.

Elevations for the pressure field and the horizontal velocity u_1 are displayed in Figures 9-12 for β=1. Computed solutions are comparable to the ones reported in [17]. However, it should be noted that the 1-jump method does behave as satisfactorily for the pressure. We also observe that there are no pressure oscillations in all presented cases. Further, the velocity streamslices of Figures 13-14 indicate that for small values of α the flow is essentially a Stokes-like flow with small counter-rotating recirculations appearing at the bottom two corners which is in agreement with some similar results found in [9] and [17]. Likewise, we observe that high values of α may lead to some oscillations as expected.

5.3. Compared performance of the 2-jump and 1-jump schemes

First of all, it is worthy to admit the difficulty of deciding a priori which of the proposed schemes would perform better than the others for a particular problem (geometry and material parameters). This can meanly come from the adopted unified theory. It seems reasonable to reckon that the constants α_1, α_2 and C_2 appearing in the structure of the convergence constant C (see (4.24) and (4.29)) play a crucial role in the behavior of the adopted discrete scheme.

Now, from the computational side, the undertaken numerical experiments allow us to draw some guidelines with respect to the appropriate number,

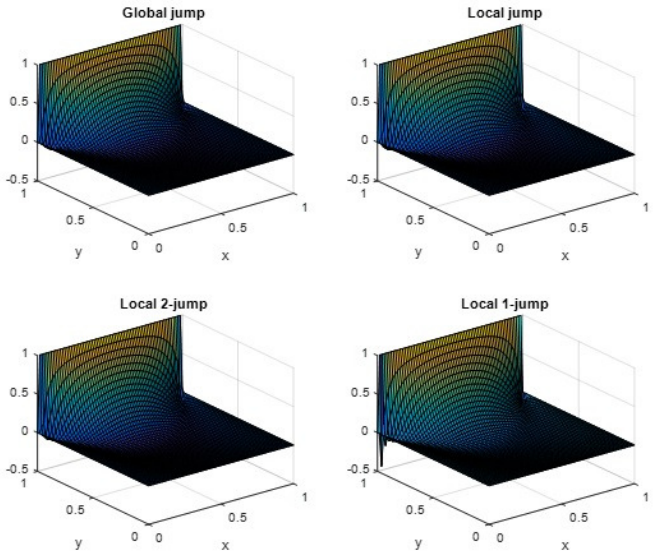

FIGURE 9. Horizontal velocity field for α=1.

position and direction of involved pressure jumps in the particular scheme. First, consider separately the two benchmark problems.

5.3.1. *Problem 1.* In this case, the H^1 velocity and L^2 pressure errors are exhibited in Tables 4-5 for the particular choice α=100 and β=1. We observe that the 2-jump schemes behave almost similarly in terms of error magnitudes. However, for the 1-jump schemes the velocity and pressure errors present discrepancies. The errors are quite comparable for the velocity while for the pressure they are more than twice larger for the two 1-jump schemes H2 and 1-jump V2. Nevertheless, both velocity and pressure errors seem to decrease according to the expected convergence rates for all schemes.

5.3.2. *Problem 2.* For this problem with non-smooth solution, the six proposed schemes are again compared using the finest grid GR5 with the parameters α=100 and β=1. The profiles of the horizontal discrete velocity u_1 along the centerline ($x = 0.5$) are plotted against that of the local jump technique, as depicted in Figure 15. Likewise, the discrete pressure profiles on the highest computed pressure level (y^*) of the cavity are displayed in Figure 16. Note that in every situation, the profiles of the local jump scheme are used as references. We observe that the agreement is quite impressive for the discrete velocity as all profiles seem to coincide. As for the discrete pressure the behavior of both local 2-jump schemes appears to be similar, whereas the local 1-jump schemes

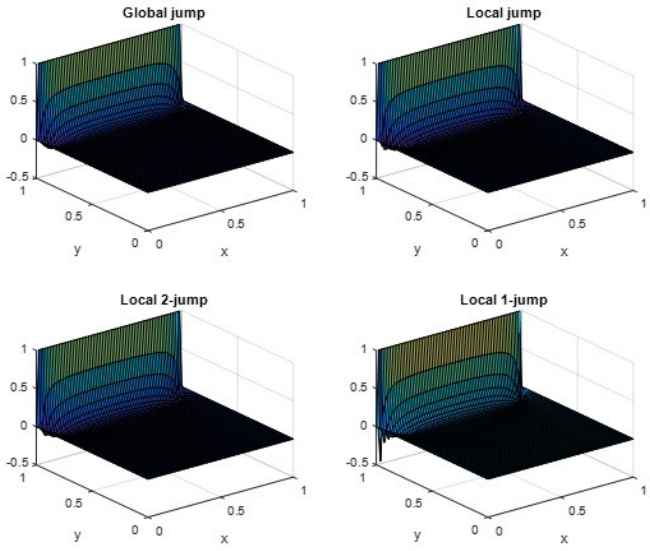

FIGURE 10. Horizontal velocity field for α=1000.

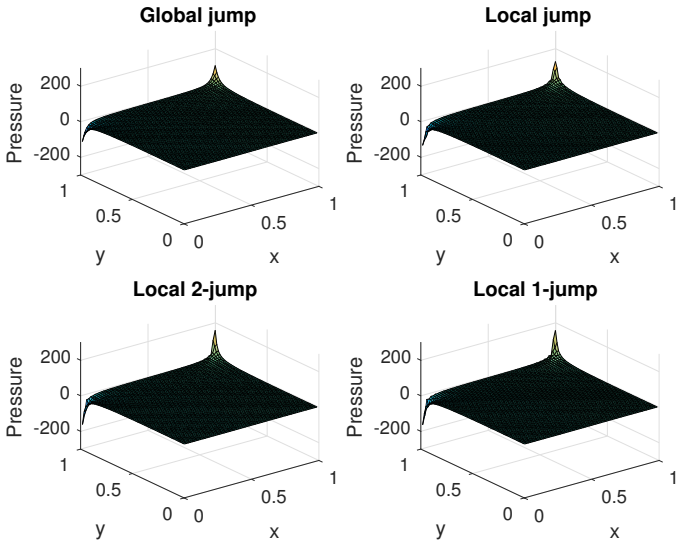

FIGURE 11. Pressure field for α=1.

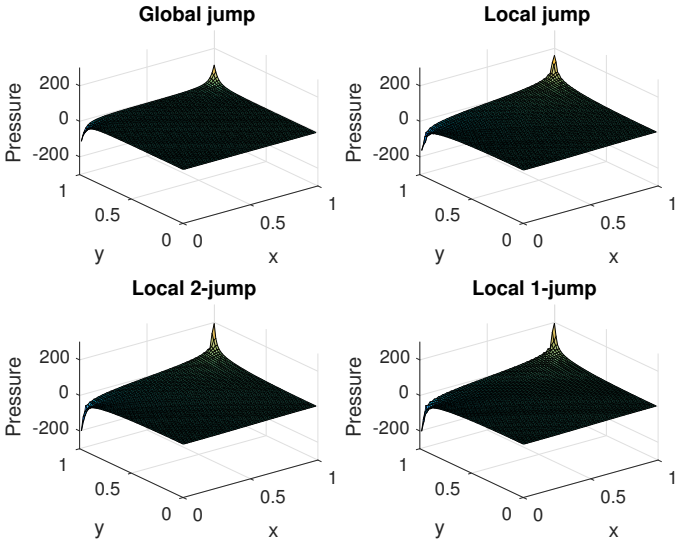

FIGURE 12. Pressure field for α=1000.

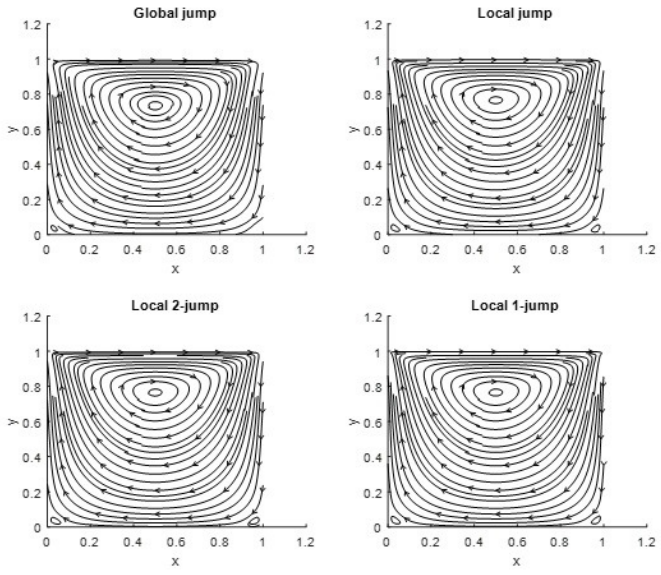

FIGURE 13. Exponential distributed streamslices plot for α=1.

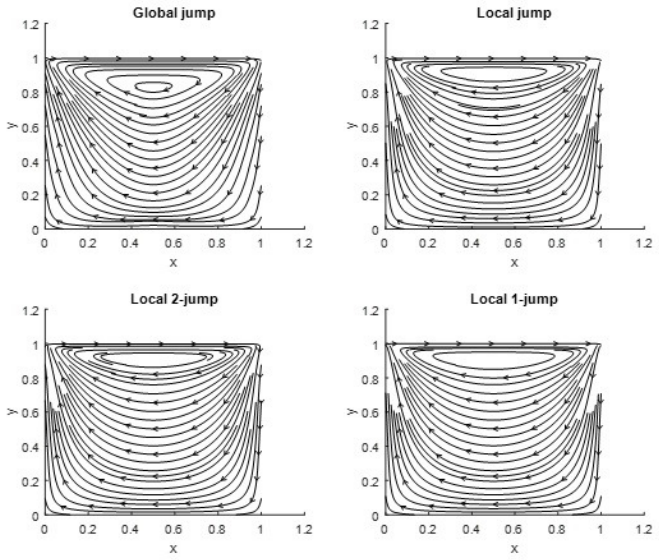

FIGURE 14. Exponential distributed streamslices plot for α=1000.

TABLE 4. Comparative behavior of $\|\mathbf{u} - \mathbf{u}_h\|_1$ for α=100 and β=1.

$1/h$	**2-jp H**	**2-jp V**	**1-jp H1**	**1-jp H2**	**1-jp V1**	**1-jp V2**
2	0.205548	0.210018	0.203715	0.246556	0.202647	0.247435
4	0.113239	0.108184	0.105926	0.131609	0.105901	0.131623
8	0.064075	0.053867	0.054042	0.066948	0.053715	0.066809
16	0.034615	0.026905	0.027059	0.033569	0.026980	0.033522
32	0.017823	0.013469	0.013523	0.016788	0.013511	0.016780
64	0.008994	0.006739	0.006760	0.008394	0.006759	0.008393
128	0.004510	0.003370	0.003380	0.004197	0.003380	0.004197
256	0.002257	0.001685	0.001690	0.002099	0.001690	0.002099
512	0.001129	0.000843	0.000845	0.001050	0.000845	0.001049

appear to be more affected by the choice of the jump. Some discrepancies occur especially in the close neighborhood of top corners where the considered problem is known to have singularity. Here, the same point is made regarding the 2-jump schemes.

5.3.3. *Useful computational guidelines.* In a general situation, it is not so straightforward to decide which scheme would behave better. Undoubtedly, this should depend on problem data and geometry. However, from the above

TABLE 5. Comparative behavior of $\|p - p_h\|_0$ for α=100 and β=1.

$1/h$	**2-jp H**	**2-jp V**	**1-jp H1**	**1-jp H2**	**1-jp V1**	**1-jp V2**
2	0.839352	0.586335	1.064232	2.209492	1.064232	2.209492
4	0.209152	0.264863	0.372040	0.652436	0.371610	0.652866
8	0.055210	0.086260	0.106325	0.181878	0.097789	0.190435
16	0.021657	0.029595	0.033910	0.066582	0.030738	0.069760
32	0.010297	0.012029	0.013135	0.029839	0.012237	0.030737
64	0.005851	0.006132	0.005544	0.014191	0.005308	0.015426
128	0.002612	0.002700	0.002796	0.007217	0.002736	0.007277
256	0.001318	0.001340	0.001372	0.003610	0.001357	0.003626
512	0.000663	0.000668	0.000681	0.001808	0.000677	0.001811

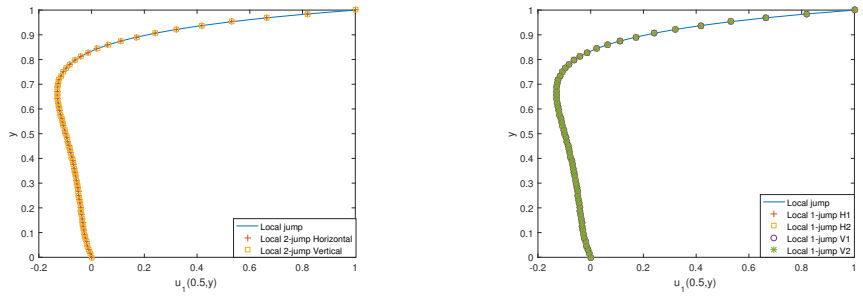

FIGURE 15. Comparative horizontal velocity profiles of the local 2-jump and 1-jump schemes for α=100 and β=1.

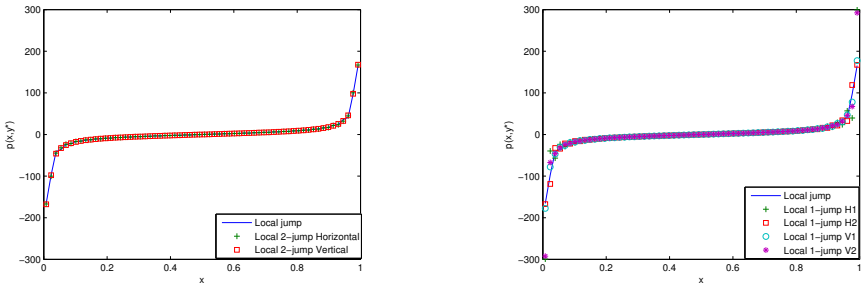

FIGURE 16. Comparative pressure profiles of the local 2-jump and 1-jump schemes for α=100 and β=1.

arguments, it is legitimate to assert that the 2-jump schemes are undisputably superior in terms of both velocity and pressure, and behave even better than

the original local jump scheme. On the other hand, the 1-jump schemes cannot be entirely discarded especially because of the sparseness of involved stabilization matrices. This could be an advantage in a possible merger within standard engineering mathematical codes.

6. Conclusion

In this work, the local jump stabilization method introduced in [15] and [21] has been first extended to the generalized Stokes problem and then reduced computationally attractive methods have been introduced, analyzed and tested on benchmark problems. Although the proposed schemes seem not competitive for extremely large values of α, but they can constitute good alternatives for moderately large values of this parameter. It is expected that their combined application with adaptive grids could be a lot better. Furthermore, there is an obvious generalization to the equivalent three-dimensional case. As future work, it would be nice to continue the development of the present stabilization techniques so as to merge the procedure within existing fluid flow packages. Research remains also to be done in further extending their applicability to the Oseen and to the fully nonlinear Navier-Stokes equations.

Acknowledgement. The authors would like to express their sincere gratitude to the anonymous referees for their careful reading of the manuscript, several valuable comments and suggestions for its improvement.

References

[1] M. Ainsworth, G. R. Barrenechea, and A. Wachtel, *Stabilization of high aspect ratio mixed finite elements for incompressible flow*, SIAM J. Numer. Anal. **53** (2015), no. 2, 1107–1120. https://doi.org/10.1137/140972755

[2] J. M. Boland and R. A. Nicolaides, *On the stability of bilinear-constant velocity-pressure finite elements*, Numer. Math. **44** (1984), no. 2, 219–222. https://doi.org/10.1007/BF01410106

[3] ———, *Stable and semistable low order finite elements for viscous flows*, SIAM J. Numer. Anal. **22** (1985), no. 3, 474–492. https://doi.org/10.1137/0722028

[4] F. Brezzi and J. Pitkäranta, *On the stabilization of finite element approximations of the Stokes equations*, in Efficient solutions of elliptic systems (Kiel, 1984), 11–19, Notes Numer. Fluid Mech., **10**, Friedr. Vieweg, Braunschweig, 1984. https://doi.org/10.1007/978-3-663-14169-3_2

[5] E. Burman and P. Hansbo, *A unified stabilized method for Stokes' and Darcy's equations*, J. Comput. Appl. Math. **198** (2007), no. 1, 35–51. https://doi.org/10.1016/j.cam.2005.11.022

[6] J. Cahouet and J.-P. Chabard, *Some fast 3D finite element solvers for the generalized Stokes problem*, Internat. J. Numer. Methods Fluids **8** (1988), no. 8, 869–895. https://doi.org/10.1002/fld.1650080802

[7] Ph. Clément, *Approximation by finite element functions using local regularization*, Rev. Française Automat. Informat. Recherche Opérationnelle Sér. **9** (1975), no. R-2, 77–84. https://doi.org/10.1051/m2an/197509R200771

[8] M. Crouzeix and P.-A. Raviart, *Conforming and nonconforming finite element methods for solving the stationary Stokes equations. I*, Rev. Française Automat. Informat.

Recherche Opérationnelle Sér. Rouge **7** (1973), no. R-3, 33–75. https://doi.org/10.1051/m2an/197307R300331

[9] H. C. Elman, D. J. Silvester, and A. J. Wathen, *Finite elements and fast iterative solvers*: *with applications in incompressible fluid dynamics*, Numerical Mathematics and Scientific Computation, Oxford University Press, New York, 2005. http://doi.org/10.1093/acprof:oso/9780199678792.001.0001

[10] F. Ghadi, V. Ruas, and M. Wakrim, *Finite element solution of a stream function-vorticity system and its application to the Navier Stokes equations*, Appl. Math. **4** (2013), 257–262. http://dx.doi.org/10.4236/am.2013.41A039

[11] V. Girault and P.-A. Raviart, *Finite element methods for Navier-Stokes equations*, Springer Series in Computational Mathematics, **5**, Springer-Verlag, Berlin, 1986. https://doi.org/10.1007/978-3-642-61623-5

[12] Y. He, J. Li, and X. Yang, *Two-level penalized finite element methods for the stationary Navier-Stoke equations*, Int. J. Inf. Syst. Sci. **2** (2006), no. 1, 131–143. http://www.math.ualberta.ca/ijiss/SS-Volume-2-2006/No-1-06/SS-06-01-16.pdf

[13] S. Hong, K. Kim, and S. Lee, *Modified cross-grid finite elements for the Stokes problem*, Appl. Math. Lett. **16** (2003), no. 1, 59–64. https://doi.org/10.1016/S0893-9659(02)00144-1

[14] T. J. R. Hughes and L. P. Franca, *A new finite element formulation for computational fluid dynamics. VII. The Stokes problem with various well-posed boundary conditions*: *symmetric formulations that converge for all velocity/pressure spaces*, Comput. Methods Appl. Mech. Engrg. **65** (1987), no. 1, 85–96. https://doi.org/10.1016/0045-7825(87)90184-8

[15] N. Kechkar and D. Silvester, *Analysis of locally stabilized mixed finite element methods for the Stokes problem*, Math. Comp. **58** (1992), no. 197, 1–10. https://doi.org/10.2307/2153016

[16] J. Li, J. Wang, and X. Ye, *Superconvergence by L^2-projections for stabilized finite element methods for the Stokes equations*, Int. J. Numer. Anal. Model. **6** (2009), no. 4, 711–723. https://doi.org/10.1007/s11432-009-0036-6

[17] K. Nafa, *Improved local projection for the generalized Stokes problem*, Adv. Appl. Math. Mech. **1** (2009), no. 6, 862–873. https://doi.org/10.4208/aamm.09-m09s07

[18] R. L. Sani, P. M. Gresho, R. L. Lee, and D. F. Griffiths, *The cause and cure* (?) *of the spurious pressures generated by certain FEM solutions of the incompressible Navier-Stokes equations. I*, Internat. J. Numer. Methods Fluids **1** (1981), no. 1, 17–43. https://doi.org/10.1002/fld.1650010104

[19] R. L. Sani, P. M. Gresho, R. L. Lee, D. F. Griffiths, and M. Engelman, *The cause and cure* (!) *of the spurious pressures generated by certain FEM solutions of the incompressible Navier-Stokes equations. II*, Internat. J. Numer. Methods Fluids **1** (1981), no. 2, 171–204. https://doi.org/10.1002/fld.1650010206

[20] Y. Shang, *A parallel finite element algorithm for simulation of the generalized Stokes problem*, Bull. Korean Math. Soc. **53** (2016), no. 3, 853–874. https://doi.org/10.4134/BKMS.b150384

[21] D. J. Silvester and N. Kechkar, *Stabilised bilinear-constant velocity-pressure finite elements for the conjugate gradient solution of the Stokes problem*, Comput. Methods Appl. Mech. Engrg. **79** (1990), no. 1, 71–86. https://doi.org/10.1016/0045-7825(90)90095-4

[22] R. Stenberg, *Analysis of mixed finite elements methods for the Stokes problem*: *a unified approach*, Math. Comp. **42** (1984), no. 165, 9–23. https://doi.org/10.2307/2007557

Alima Chibani
Department of Mathematics
Faculty of Exact Sciences
University Frères Mentouri
Constantine 25000, Algeria
Email address: almchibani@gmail.com

Nasserdine Kechkar
Department of Mathematics
Faculty of Exact Sciences
University Frères Mentouri
Constantine 25000, Algeria
Email address: kechkar.nasserdine@umc.edu.dz